



Share Your Innovations through JACS Directory

Journal of Nanoscience and Technology

Visit Journal at <http://www.jacsdirectory.com/jnst>

ISSN: 2455-0191

Optical and Structural Investigation of Mg²⁺ doped ZnO Nanoparticles using *Gymnema sylvestre* and *Mangifera indica* Leaves ExtractsM. Karthikeyan¹, A. Jafar Ahamed^{1,*}, P. Vijaya Kumar²¹Post Graduate and Research Department of Chemistry, Jamal Mohamed College (Autonomous), Tiruchirappalli - 620 020, Tamil Nadu, India.²Department of Chemistry, Asan College of Arts and Science, Karur- 639 003, Tamil Nadu, India.

ARTICLE DETAILS

Article history:

Received 07 January 2019

Accepted 27 January 2019

Available online 04 February 2019

Keywords:

Green Synthesis

Zinc Oxide

*Gymnema sylvestre**Mangifera indica*

ABSTRACT

In green nanotechnology, plant is used for the synthesis of nanoparticles which are gaining considerable interest among researchers as an eco-friendly alternative to conventional physical and chemical methods, as this approach eliminates the use of toxic chemicals. The present study describes the synthesis of Mg²⁺ (magnesium) doped zinc oxide (ZnO) nanoparticles (NPs) M1 using leaves extract of *Gymnema sylvestre* (*G. sylvestre*) belonging to *Asclepiadaceae* family and M2 using *Mangifera indica* (*M. indica*) belonging to *Anacardiaceae* family as reducing as well as capping agents. The obtained Mg²⁺ doped ZnO NPs (M1 and M2) were characterized by X-ray diffraction (XRD) studies, field emission scanning electron microscopy (FESEM), elemental analysis (EDAX), Fourier transform infrared spectroscopy (FTIR), UV-vis spectroscopy and photoluminescence (PL) spectra.

1. Introduction

The metal oxide NPs are synthesized by green method using biological material as the reducing as well as stabilizing agents has attracted a lot of considerable attention in the field of biomedical sectors and pharmaceuticals as compared to the toxic physical and chemical methods due to the usage of non-toxic, safe reagents and eco-friendly during the biosynthesis methods [1–5].

Since, ZnO NPs having multifunctional morphology, tunable, photonic and spintronic properties and it is used as the most exploited n-type semiconducting metal oxide materials. It is characterized by a wide direct band gap of 3.37 eV and a high excitation energy of 60 meV. Due to these characteristics, ZnO NPs is widely used in numerous devices, including gas sensing, optoelectronics and surface acoustic wave devices. [6–11]. These nanoparticles can be synthesized by different techniques that include chemical precipitation, sol-gel, spray pyrolysis, thermal decomposition, electrochemical and photochemical reduction techniques [12, 13]. However, most of these conventional methods involve sophisticated equipment, rigorous procedures, tedious processes and high-cost organic solvents that could generate toxic wastes [13, 14]. Thus, there is an increasing need to develop eco-friendly synthesis methods that do not require the use of substances with adverse consequences on the environment and human health.

In this present study, we focused on the preparation of Mg²⁺ doped ZnO NPs by green method using *G. sylvestre* and *M. indica* leaves extract as reductant and stabilizing agent. The structural and optical properties of synthesized NPs have been investigated.

2. Experimental Methods

2.1 Preparation of Mg²⁺ doped ZnO NPs by using *G. sylvestre* and *M. indica* Leaves Extracts

15 g of finely chopped *G. sylvestre* leaves were weighed, then 150 mL of double distilled water was added and boiled at 80 °C for 1 h, the obtained extract was filtered using Whatman No.1 filter paper and the filtrate was collected in 250 mL Erlenmeyer flask. Thereafter, 0.090 M Zn(NO₃)₂·6H₂O

and 0.010 M Mg(NO₃)₂·6H₂O solution was added into 150 mL of *G. sylvestre* leaves extract and it was stirred constantly at 80 °C for 6 hours. A dull yellow colour precipitate was obtained, further the precipitate was dried at 120 °C for 6 hours. The obtained Mg²⁺ doped ZnO NPs (M1) was annealed at 700 °C for 6 hours. The same procedure was followed for the preparation of Mg²⁺ doped ZnO NPs (M2) using *M. indica* leaves extracts. Fig. 1 shows the schematic diagram of synthesized Mg²⁺ doped ZnO NPs using *G. sylvestre* and *M. indica* leaves extracts.

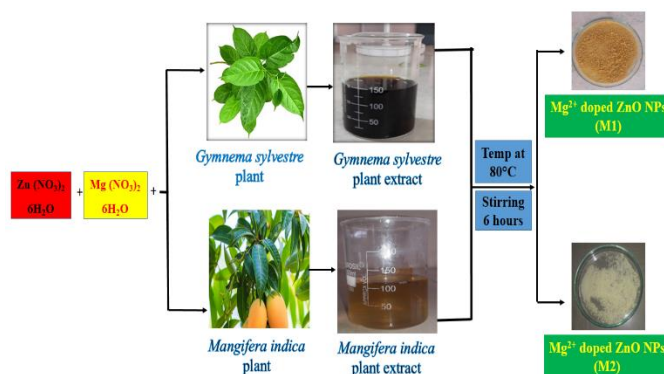


Fig. 1 Schematic diagram for the formation of M1 and M2 samples

2.2 Characterization Studies

The phase purities of the synthesized NPs were determined by X-ray diffractometer (Model: X'PERT PRO PAN analytical). The morphological features of the sample were measured by field emission scanning electron microscopy (Model: Carl Zeiss 55) with EDAX (ultras). The vibrational frequency was measured by Fourier transform infra-red spectroscopy (Perkin-Elmer). The absorption spectrum of the sample was measured on Perkin-Elmer (Lambda 35). The PL emission study of the sample was carried out using Horiba Jobin YVON spectrofluorometer (model: FLUOROMAX-4, 450 W high pressure Xenon lamp as the excitation source, photomultiplier at a range 325–550 nm).

*Corresponding Author: agjafar@yahoo.co.in (A. Jafar Ahamed)

3. Results and Discussion

3.1 X-Ray Diffraction Studies

Fig. 2(a-b) show the XRD patterns of M1 and M2 synthesized by using *G. sylvestre* and *M. indica* leaves extract. The XRD peaks are appeared at angles (2θ) of 32.006°, 34.686° and 36.489° corresponding to (100), (002) and (101) planes of ZnO NPs respectively. Similarly, other peaks found at angles (2θ) of 47.812, 56.798, 63.096, 68.15, 69.26, 72.84 and 77.15 are corresponding to (102), (110), (103), (112), (201), (004) and (202) planes of ZnO NPs respectively. The standard diffraction peaks show that the hexagonal wurtzite structure of ZnO NPs with space group of p63mc. It is also confirmed by the JCPDS data (card No: 361451). The ionic radii of Mg^{2+} 0.66 Å. Hence there is no impurity phase found in both synthesized NPs.

The average crystallite size of the synthesized ZnO NPs was estimated from X-ray line broadening of the diffraction peaks using Debye Scherrer's relation.

$$\text{Average crystallite size (D)} = \frac{0.9 \lambda}{\beta \cos \theta} \quad (1)$$

where D is the crystallite size, λ is the wavelength (1.5406 Å CuK α), θ is the Bragg diffraction angle and β is the full width at half maximum (FWHM). The average crystallite sizes of 38 nm for M1 sample synthesized by using *G. sylvestre* whereas 41 nm for M2 synthesized using *M. indica* leaves extracts. From these results, M1 sample showed decrease in the particle size due to the influence of *G. sylvestre* plant extract. Both the samples exhibit peaks in the same range but M1 sample found to exhibit sharp peak [15].

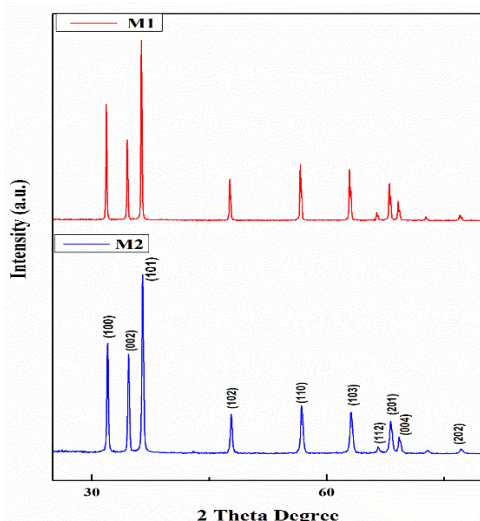


Fig. 2 XRD pattern of M1 and M2 samples

3.2 Field Emission Scanning Electron Microscopy (FESEM) studies

The surface morphologies of M1 and M2 samples synthesized using *G. sylvestre* and *M. indica* leaves extract are shown in Fig. 3(a-b). From the FESEM images, the M1 and M2 samples form a spindle and spherical like nanostructures. The size of the particles obtained as 37 nm for M1 sample synthesized by using *G. sylvestre* while it where 41nm for M2 sample synthesized using *M. indica* leaves extract.

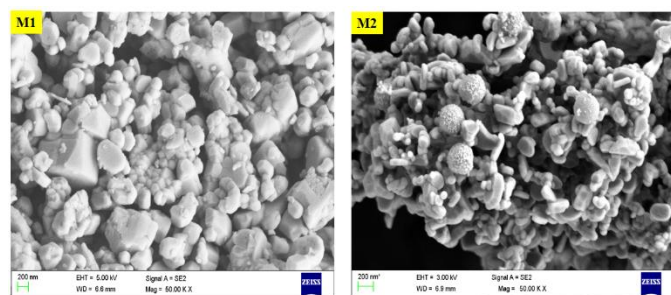


Fig. 3 FESEM images M1 and M2 samples

3.3 Energy Dispersive Analysis of X-Ray (EDAX) Studies

The elemental compositional analysis of M1 and M2 using *G. sylvestre* and *M. indica* leaves extract were carried out using EDAX studies. The <https://doi.org/10.30799/jnst.205.19050107>

typical EDAX spectrum of the M1 and M2 are shown in Fig. 4(a-b). The atomic weight percentage of the synthesized sample is Zn=76.66, O=21.30 and Mg=2.04 for M1 sample synthesised using *G. sylvestre* whereas Zn=78.06, O=19.30 and Mg=2.34 for M2 sample using *M. indica* leaves extract.

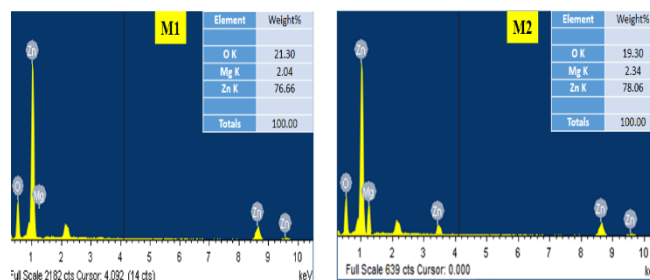


Fig. 4 EDAX spectra of M1 and M2 samples

3.4 Fourier Transform Infrared (FTIR) Studies

The FT-IR spectra of M1 and M2 samples using *G. sylvestre* and *M. indica* leaves extracts are shown in Fig. 5(a-b). The stretching frequencies of the obtained NPs where analysed by FT-IR in the range from 400 to 4000 cm^{-1} at room temperature. The FT-IR spectra contains several characteristic bands. The absorption peak appeared at 3432 cm^{-1} corresponds to the stretching vibration of the O-H band. This absorption peak is appeared due to the surface absorption of water molecules in both synthesized NPs [16]. The peaks appear around at 1628 cm^{-1} and 1642 cm^{-1} are due to H-O-H bending vibration frequencies which is assigned to a small amount of moisture H_2O molecules observed on the surface of ZnO NPs [17]. The weak metal-oxygen (Zn-O) vibration frequency is observed at 871 cm^{-1} for ZnO NPs. The medium intense peak appeared at 464 cm^{-1} was recognized as the Zn-O stretching band.

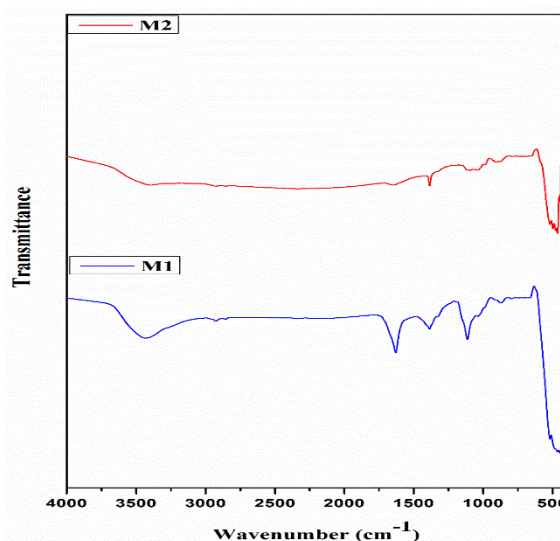


Fig. 5 FT-IR spectra of M1 and M2 samples

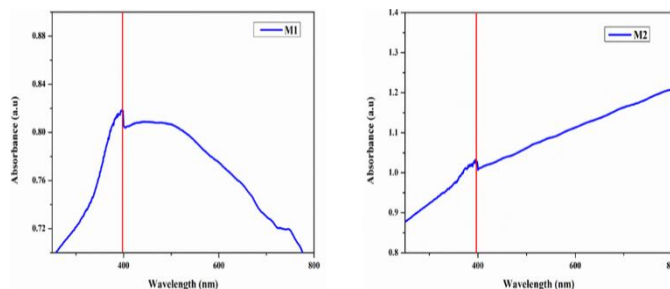


Fig. 6 Absorption spectra of M1 and M2 samples

3.5 UV-Vis Absorption Spectroscopy

UV-visible optical absorption spectra were recorded at room temperature in the wavelength range 350–800 nm and shown in Fig. 6(a-b). The samples were uniformly dispersed in distilled water, followed by ultra-sonification for 15–20 min before recording UV-Vis spectra. From the absorption spectra, the absorption peaks are found at 398 nm for M1 sample synthesized by using *G. sylvestre* whereas 395 nm for synthesized

for M2 sample using *M. indica* leaves extracts, which can be attributed to the photo excitation of electrons from valence band to conduction band [18].

3.6 Photoluminescence (PL) Studies

The photoluminescence spectra of synthesized M1 and M2 samples recorded with the excited wavelength of 385 nm are shown in Fig. 7(a–b). The PL emissions are observed for M1 and M2 sample covering from the very short wavelength of 350 nm to long wavelength 600 nm. The emission spectra of the M1 sample is having four peaks at 365, 390, 402 and 423 nm synthesized using *G. sylvestre* whereas six peaks at 384, 411, 444, 458, 479 and 521 nm for M2 sample synthesized using *M. indica* leaves extract respectively. It is due to the violet emissions, blue emissions, blue-green emission and green emission respectively.

The lowest wavelengths of UV emission peaks are observed at 365, 384 and 390 nm, which correspond to the near-band emission (NBE) of Mg²⁺ doped ZnO NPs. The four violet emissions centered at 402, 411, 423 and 444 nm are ascribed to an electron transition from a shallow donor level of the natural zinc interstitials to the top level of the valence band [19]. The blue green emission observed at 452 and 479 nm are ascribed to the transition between the oxygen and interstitial oxygen vacancies [20]. Finally, green emission observed at 521 nm, corresponds to the singly ionized oxygen vacancies [21, 22].

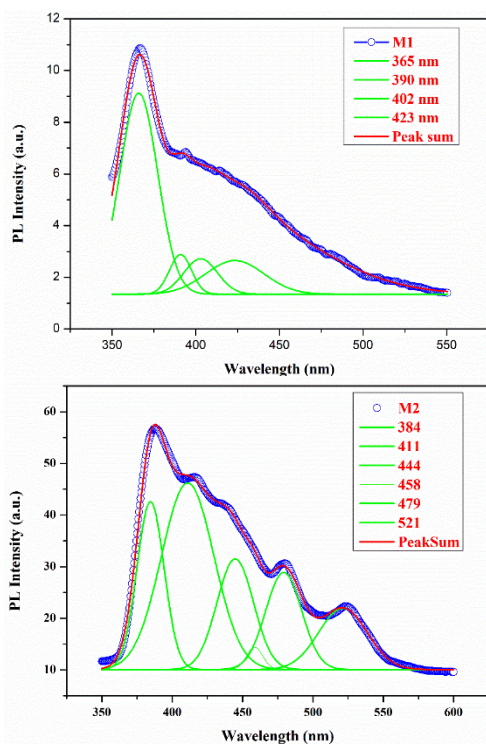


Fig. 7 PL emissions spectra of M1 and M2 samples

4. Conclusion

The Mg²⁺ doped ZnO NPs were successfully synthesized by green method using *Gymnema sylvestre* and *Mangifera indica* leaves extract as reducing agents. The X-ray diffraction results confirmed that the prepared Mg²⁺ doped ZnO NPs (M1 and M2) have hexagonal wurtzite structure. The morphologies of nanoparticles were confirmed by FESEM analysis. The elemental composition of the synthesized NPs were identified by EDAX spectra. Using the recorded FT-IR spectra, the various vibrational frequencies were assigned for the both synthesized samples. The UV-Vis spectrum showed the absorption peak found at 398 and 395 nm for M1 and M2 samples synthesized by using *G. sylvestre* and *M. indica* leaves

extract respectively. PL spectra showed that doping materials altered the band emission, which is due to zinc vacancy, oxygen vacancy and surface defects. This method stands out primarily due to the fact that it is eco-friendly and shuts down the demerits of conventional physical and chemical methods. The synthesized NPs are anticipated to have extensive applications in various industrial features.

Acknowledgements

The authors are thankful to the members of Management committee and Principal of Jamal Mohamed College for providing necessary facilities.

References

- [1] M. Moritz, M.G. Moritz, The newest achievements in synthesis, immobilization and practical applications of antibacterial nanoparticles, Chem. Eng. J. 228 (2013) 596–613.
- [2] P. Rajiv, S. Rajeshwari, R. Venkatesh, Bio-fabrication of zinc oxide nanoparticles using leaf extract of *Parthenium hysterophorus* L. and its size-dependent antifungal activity against plant fungal pathogens, Spectrochim. Acta A 112 (2013) 384–387.
- [3] S.D. Caruthers, S.A. Wickline, G.M. Lanza, Nanotechnological applications in medicine, Curr. Opin. Biotechnol. 18 (2007) 26–30.
- [4] D. Nath, P. Banerjee, Green nanotechnology - a new hope for medical biology, Environ. Toxicol. Pharmacol. 36 (2013) 997–1014.
- [5] H.A. Salam, P. Rajiv, M. Kamaraj, P. Jagadeeswaran, S. Gunalan, R. Sivaraj, Plants: green route for nanoparticle synthesis, Int. Res. J. Biol. Sci. 1(5) (2012) 85–90.
- [6] K. Ellmer, A. Klein, B. Rech, Transparent conductive zinc oxide, Springer Series in Materials Science, Germany, 2008.
- [7] U. Ozgur, Y.I. Alivov, C. Liu, A. Teke, M.A. Reshchikov, et al., A comprehensive review of ZnO materials and devices, Appl. Phys. 98 (2005) 041301-1-103.
- [8] F. Kaminsky, Mineralogy of the lower mantle: A review of 'super-deep' mineral inclusions in diamond, Earth. Sci. Rev. 110 (2012) 127-147.
- [9] G. Eranna, B.C. Joshi, D.P. Runthala, R.P. Gupta, Oxide materials for development of integrated gas sensors - A comprehensive review, Crit. Rev. Solid State Mater. Sci. 29 (2004) 111-188.
- [10] S. Kalusniak, S. Sadofev, J. Puls, F. Henneberger, ZnCdO/ZnO - a new heterosystem for green-wavelength semiconductor lasing, Laser Photonics Rev. 3 (2009) 233-242.
- [11] Y. Li, J. Z. Zhang, Hydrogen generation from photo electrochemical water splitting based on nanomaterials, Laser Photonics Rev. 4 (2010) 517-528.
- [12] K. Elumalai, S. Velmurugan, S. Ravi, V. Kathiravan, S. Ashokkumar, Green synthesis of zinc oxide nanoparticles using *Moringa oleifera* leaf extract and evaluation of its antimicrobial activity, Spectrochim Acta A Mol. Biomol. Spectros. 143 (2015) 158-164.
- [13] P. Nagajyothi, S. Cha, I. Yang, T. Sreekanth, K.J. Joong Kim, Antioxidant and anti-inflammatory activities of zinc oxide nanoparticles synthesized using *Polygala tenuifolia* root extract, Photochem. Photobiol. 146 (2015) 10-17.
- [14] D. Suresh, P. Nethravathi, P. Udayabhanu, H. Rajanaika, H. Nagabhushana, S. Sharma, *Tinospora cordifolia* mediated facile green synthesis of cupric oxide nanoparticles and their photocatalytic, antioxidant and antibacterial properties, Mater. Sci. Semicond. Process. 31 (2015) 446-454.
- [15] A. Vanaja, K. Srinivasa Rao, Effect of solvents on particle structure, morphology and optical properties of zinc oxide nanoparticle, Int. J. Adv. Mater. Sci. Eng. 4(2) (2015) 1-8.
- [16] Y. Wang, X. Liao, Z. Huang, G. Yin, J. Gu, Y. Yao, Preparation and characterization of Ni doped ZnO particles via a bio assisted process, Colloids Surf. A 372 (2010) 165-171.
- [17] Y.S. Sonawane, K.G. Kanade, B.B. Kale, R.C. Aiyer, Electrical and gas sensing properties of self-aligned copper-doped zinc oxide nanoparticles, Mater. Res. Bull. 43 (2008) 2719-2726.
- [18] M. Liu, A.H. Kitai, P. Mascher, Point defects and luminescence centres in zinc oxide and zinc oxide doped with manganese, J. Lumin. 54(1) (1992) 35-42.
- [19] X.M. Fan, J.S. Lian, L. Zhao, Y. Liu, Single violet luminescence emitted from ZnO films obtained by oxidation of Zn film on quartz glass, Appl. Sur. Sci. 252 (2005) 420-424.
- [20] N. Varghese, L.S. Panchakarla, M. Hanapi, A. Govindaraj, C.N.R. Rao, Solvothermal synthesis of nanorods of ZnO, N-doped ZnO and CdO, Mater. Res. Bull. 42 (2007) 2117-2124.
- [21] N. Kumar, A. Dorfman, J. Hahm, Fabrication of optically enhanced ZnO nanorods and microrods using novel biocatalysts, J. Nanosci. Nanotech. 5 (2005) 1915-1918.
- [22] D.M. Bagnall, X.F. Chen, M.Y. Shen, Z. Zhu, T. Goto, T. Yao, Room temperature excitonic stimulated emission from zinc oxide epilayers grown by plasma-assisted MBE, J. Cryst. Growth 184 (1998) 605-609.